On worst-case correlation length in probabilistic 3D bearing capacity assessments

Li, Yajun; Li, Jianguang; Xu, Nengxiong; Fenton, Gordon A.; Vardon, Philip J.; Hicks, Michael A.

DOI
10.1080/17499518.2022.2132262

Publication date
2022

Document Version
Final published version

Published in
Georisk

Citation (APA)
Li, Y., Li, J., Xu, N., Fenton, G. A., Vardon, P. J., & Hicks, M. A. (2022). On worst-case correlation length in probabilistic 3D bearing capacity assessments. *Georisk*, *17*(3), 543-553. https://doi.org/10.1080/17499518.2022.2132262

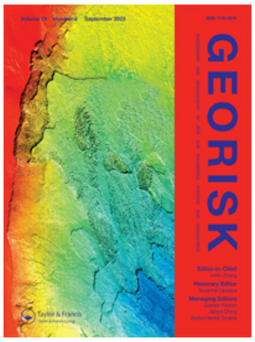

Georisk: Assessment and Management of Risk for Engineered Systems and Geohazards

ISSN: (Print) (Online) Journal homepage: https://www.tandfonline.com/loi/ngrk20

On worst-case correlation length in probabilistic 3D bearing capacity assessments

Yajun Li, Jianguang Li, Nengxiong Xu, Gordon A. Fenton, Philip J. Vardon & Michael A. Hicks

GEORISK
https://doi.org/10.1080/17499518.2022.2132262

On worst-case correlation length in probabilistic 3D bearing capacity assessments

Yajun Li [a], Jianguang Li [a,b], Nengxiong Xu [a], Gordon A. Fenton [c], Philip J. Vardon [d] and Michael A. Hicks [d]

[a]School of Engineering and Technology, China University of Geosciences, Beijing, People's Republic of China; [b]Institute of Geotechnical Engineering, Aviation Industry Corporation of China (AVIC), Beijing, People's Republic of China; [c]Department of Engineering Mathematics, Dalhousie University, Halifax, Canada; [d]Department of Geoscience and Engineering, Delft University of Technology, Delft, The Netherlands

ABSTRACT
Correlation length or scale of fluctuation (SOF) is often used as a primary parameter in defining the spatial correlation characteristics of varying soil properties. However, geotechnical site investigations are rather limited so that proper determination of correlation length is not always possible. The concept of a worst-case correlation length thus has important implications in reliability-based designs. In the case of insufficient information, the worst-case correlation length can be used to conservatively estimate the reliability or probability of failure of geotechnical structures. However, the definition of the worst-case correlation length in the literature is not very clear and has been seen in some investigations to not exist. This paper, in the context of bearing capacity of 3D spatially varying soils, investigates the worst-case correlation length based on different definitions to clarify past findings. Further analyses provide insight into practical applications, where the impact of site sampled data and realistic uncertainties are considered. Using realistic values of the coefficient of variation, and taking account of the distance at which site investigation is likely to occur from the loaded area, a worst-case SOF is identified and found to be similar using all definitions.

ARTICLE HISTORY
Received 26 December 2021
Accepted 20 September 2022

KEYWORDS
Bearing capacity; foundation; reliability; scale of fluctuation; spatial variability; square footing

1. Introduction

Soil properties vary spatially. In order to quantitatively characterise this spatial variability, a parameter is defined to statistically describe their rate of change or fluctuation in space. This so-called scale of fluctuation (SOF) (Vanmarcke 1977, 1978) is mathematically defined as the integrated area under the correlation function (Vanmarcke 1983). In geostatistics, this scale is more often referred to as the correlation length (CL), which differs from the SOF by a factor of 2 (i.e. it is half the magnitude of the SOF).

The scale of fluctuation indicates that soil properties at some point in space are only correlated to those within this scale or length. A smaller value of the scale means that soils at any spatial point are only correlated with those within a small radius. For a larger value, this means a correlated area with a larger radius around any point. In cases where a large site investigation database is available (which is perfectly possible although scarce), statistical spatial analysis can be carried out to determine the scale of fluctuation (Fenton 1999; Jaksa, Kaggwa, and Brooker 1999; Lundberg and Li 2015; De Gast, Vardon, and Hicks 2021). However, in most cases, site data are not sufficient to be able to carry out such an analysis, due largely to the limited intensity of geotechnical site investigations, which in turn is a direct result of expenditure. In such cases, if a reliability-based design is required, a range of possible values may be assumed based on local experience and as much information as one could get from other similar sites, until further improved information is available. By doing this kind of parametric/sensitivity analysis, one could possibly find a worst-case scale of fluctuation where the probability of failure of the geotechnical structure is a maximum. However, this maximum is not always observable at some intermediate value of the SOF as will be discussed later (together with the traditional factor of safety).

The concept of a worst-case SOF is attractive, since this could be used conservatively in a preliminary reliability-based design. The observation of a worst-case SOF was reported as early as Baecher and Ingra (1981), who looked at the differential settlement of a flexible footing. Later, Fenton, Paice, and Griffiths (1996) and Fenton and Griffiths (2002) found similar behaviour when investigating the differential settlement for two-footing problems, i.e. the mean absolute differential settlement has a maximum at some intermediate

CONTACT Yajun Li y.j.li@cugb.edu.cn

SOF. Interested readers are also referred to Christian and Baecher (2003). The phenomenon has since been reported for various geotechnical problems, such as draw-down in free-surface flow, exit gradient in seepage, bearing capacity, slope stability, basal heave stability and retaining wall stability, when considering soil spatial variability (Fenton and Griffiths 1996, 2008; Griffiths and Fenton 1998; Li, Hicks, and Nuttall 2015; Ching, Phoon, and Sung 2017; Puła, Pieczyńska-Kozłowska, and Chwała 2017; Li et al. 2017; Zhu, Griffiths, and Fenton 2018; Cami et al. 2020; Vessia et al. 2021).

There are generally two definitions for the so-called worst-case SOF. One is based on the mean soil response being on the most unsafe side, as in, e.g. Fenton and Griffiths (2003) and Ching, Phoon, and Sung (2017), and the other is based on the probability of failure being a maximum, as in, e.g. Fenton, Griffiths, and Williams (2005), Griffiths, Fenton, and Ziemann (2008) and Zhu, Griffiths, and Fenton (2018). For the latter definition, the probability of failure is quite often seen to be a maximum for an infinite SOF. In addition, the critical SOF may or may not be the same under these two definitions (as will be seen), since the factor of safety in stability calculations and the variance of the soil response also play important roles in calculating the probability of failure. Moreover, some studies have looked at the worst-case SOF behaviour from a theoretical point of view (e.g. Allahverdizadeh, Griffiths, and Fenton 2015; Zhu, Griffiths, and Fenton 2018), i.e. ignoring the practical ranges of coefficient of variation of soil properties and/or failure probability levels of structural performance, as well as direct use of samples in the simulations, with the exception of limited studies carried out in the context of load and resistance factor design of geotechnical structures (Fenton et al. 2003; Fenton, Griffiths, and Cavers 2005; Fenton, Zhang, and Griffiths 2007; Fenton, Griffiths, and Zhang 2008).

This paper considers the ultimate limit state (i.e. bearing capacity) of shallow foundations and is devoted to the ambiguities caused by the two definitions of the worst-case SOF and to demonstrating that they may end up being the same value for practical purposes. The question of observability of such values (i.e. under what conditions they may be observed at some intermediate value) is also discussed for the case of stability of a square footing resting on a 3D spatially varying soil. For the case when they are not so apparently observable (i.e. less pronounced) in practical terms, it is investigated if an infinite SOF should be used in reliability-based designs and how directly including samples in the analysis should end up with a different critical value of the SOF than infinity in practice.

2. Random finite element model

The worst-case SOF may be observed most easily in a structured numerical investigation using a variety of SOFs. The random finite element method (RFEM) (Fenton and Griffiths 2008) is the most common form of analysis and is therefore used here. The method requires the use of a random field. In this paper, the local average subdivision method is used (Fenton and Vanmarcke 1990) to generate random fields, as it fully accounts for spatial correlation and averaging. In reliability assessments of footing stability, the method involves generating multiple realisations of the spatial variability of soil property values and carrying out a finite element analysis (FEA) for each realisation to assess the ultimate bearing capacity (q_f). In this paper, parametric studies of square surface footings on weightless cohesive soils are carried out. The soil undrained shear strength c_u is assumed to be characterised by a lognormally distributed random field, with other parameters kept constant due to their values not significantly affecting the ultimate bearing capacity (Li et al. 2020). The correlation structure of $\ln c_u$ is characterised by a simple exponential correlation function:

$$\rho_{\ln c_u}(\tau_1,\tau_2,\tau_3)=\exp\left(-\frac{2|\tau_3|}{\theta_{\ln c_u}}-\sqrt{\left(\frac{2\tau_1}{\theta_{\ln c_u}}\right)^2+\left(\frac{2\tau_2}{\theta_{\ln c_u}}\right)^2}\right) \tag{1}$$

where τ_1, τ_2, τ_3 are the components of the separation distance vector $\boldsymbol{\tau}=\boldsymbol{x}-\boldsymbol{x}'$ between two spatial points, $\boldsymbol{x}$ and $\boldsymbol{x}'$, and $\theta_{\ln c_u}$ is the isotropic SOF (i.e. the same in the vertical and two horizontal directions). For anisotropic correlation, different values of the SOF (i.e. $\theta^v_{\ln c_u}$ and $\theta^h_{\ln c_u}$) should be used in the vertical (τ_3) and horizontal (τ_1 and τ_2) directions.

Table 1 shows the input parameters for the Monte Carlo (MC) simulation. The mean strength is taken as $\mu_{c_u}=100$ kPa. The coefficient of variation (COV, $v_c=\sigma_{c_u}/\mu_{c_u}$, where σ_{c_u} is the standard deviation of the undrained shear strength) is chosen based on the recommended range of 0.1–0.5 for clays (Phoon and Kulhawy 1999; Hicks and Samy 2002), although some exceptionally high values are also considered. Seven cases corresponding to different values of the SOF, $\theta_{\ln c_u}$, have been investigated; each case involves the generation of $N=600$ realisations of the shear strength

Table 1. Input parameters used in this study.

Parameter	Value	Units
μ_{c_u}	100	kPa
v_c	0.1, 0.2, 0.5, 1.0, 2.0	–
$\theta_{\ln c_u}$	0.1, 0.5, 1.0, 2.0, 4.0, 8.0, 50	m

random field and subsequent nonlinear finite element analysis of the bearing capacity (Smith and Griffiths 2005; Li et al. 2020). The soil behaviour is modelled by a Tresca model. The three input material parameters for a Tresca soil are the Young's modulus E, Poisson's ratio ν and undrained shear strength c_u. In this study, c_u is treated as a random field while E and ν are kept constant (i.e. $E = 100,000\,\mathrm{kN/m^2}$ and $\nu = 0.3$), since earlier deterministic evaluations showed that the deformation parameters do not significantly affect the ultimate bearing capacity (Li et al. 2020, 2021). To aid numerical stability and efficiency in the undrained analysis, a Poisson's ratio of 0.3 was used instead of 0.5, which would be expected for undrained cases (Li et al. 2021). Random fields of E and/or ν may also be generated and used, cross-correlated to c_u. However, this was not included due to primarily the low impact, and secondly the increased complexity of the analysis, without sufficient supporting data for the use of correlations or different scales of fluctuations. The paper aims to clarify the worst-case SOF in its simplest form at the ultimate limit state of a square footing, avoiding complicating the matter with possible various combinations of SOFs for different parameters.

Figure 1 shows the 3D finite element (FE) mesh discretisation used in the following analyses. The footing width considered is $B = 1.0$ m. The boundary conditions are a fixed base and rollers on the two (front and back) x–z and two (left and right) y–z faces preventing displacement perpendicular to the faces. The rough footing conditions are simulated by restraining the horizontal displacements (i.e. in the x and y directions) of the nodes representing the footing. The mesh comprises 3200 14-node hexahedral elements ($20 \times 20 \times 8$). Each element has dimensions of $0.25 \times 0.25 \times 0.25$ m. Thus, the problem domain has a size of $5 \times 5 \times 2$ m. This mesh density yields a deterministic bearing capacity factor of $N_c' = 7.389$, whereas a finer mesh with $40 \times 40 \times 16$ elements gives $N_c' = 6.517$, which is a closer bearing capacity factor to the empirical value of 1.2×5.7 (Meyerhof 1951). An efficient procedure was used to obtain a series of bearing capacity values q_f that are effectively equivalent to analysing the same problem with a finer mesh (Li et al. 2020); that is, normalising the ensemble of q_f values (from an MC simulation) with respect to the deterministic value calculated using the coarse mesh, and then scaling the normalised values by the deterministic value calculated using the finer mesh. In this way, the finite element analysis of the finer mesh problem needs only be run once for the deterministic case. In the following, q_f from each realisation is nondimensionalised with respect to the mean undrained shear strength μ_{c_u}, to give a stochastic bearing capacity factor $M_c = q_f/\mu_{c_u}$. The normalisation and scaling procedure has been verified based on $N = 100$ MC realisations for $\mathrm{COV} = 0.2$ (Li et al. 2020) and $\mathrm{COV} = 0.5$ (Li et al. 2021), i.e. by comparing the ensemble of M_c values from the finer mesh (0.125 m) with the ensemble of M_c values from the coarse mesh (0.25 m) scaled by 6.517/7.389. This is shown in Figure 2, where the results cluster closely around the 1:1 line, indicating the effectiveness of the procedure.

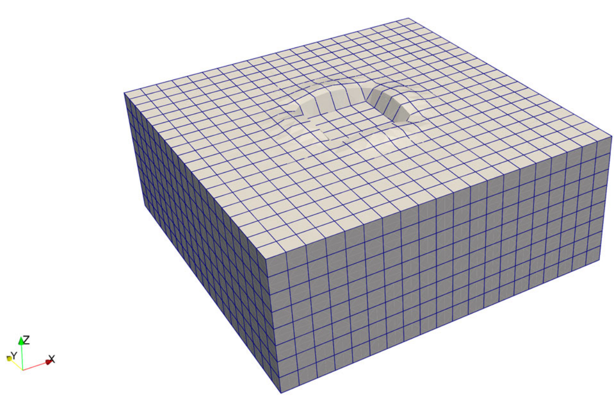

Figure 1. Deformed finite element mesh ($5 \times 5 \times 2$ m) for a square footing (deformation enlarged by a factor of 3 and footing width $B = 1.0$ m).

In the RFEM analysis, the generated random field cell values are mapped onto the finite element mesh at the Gauss point level so as to adequately represent the spatial variability (Spencer 2007; Huang and Griffiths 2015; Tabarroki and Ching 2019) (each finite element has $2 \times 2 \times 2$ integration points). Figure 3 shows a typical realisation of $\ln c_u$ with $\theta_{\ln c_u} = 2.0$ m. For the case of $\theta = 0.1$ m, the mesh size may not be small enough to take proper account of the spatial variability (and thereby to generate a more realistic failure surface) in the finite element analysis. A general rule of thumb would be that the ratio of random cell size to the SOF should be in the range of 0.1–0.25, depending the tolerance criterion (see Spencer 2007; Huang and Griffiths 2015; Tabarroki and Ching 2019). In the RFEM simulation, mapping the random cell values to the Gaussian point level in the finite elements ensures the final failure mechanism being modelled more appropriately through a more realistic representation of the soil spatial variability. Also, although a 0.25 m mesh size is used, it has been proven in Figure 2 that the results can be scaled to the results based on a mesh size of 0.125 m (this partly solves the finite element discretisation error). Through mapping onto the Gaussian points within each element, this means an equivalent random cell size of 0.0625 m is used, which is roughly half of the smallest SOF used.

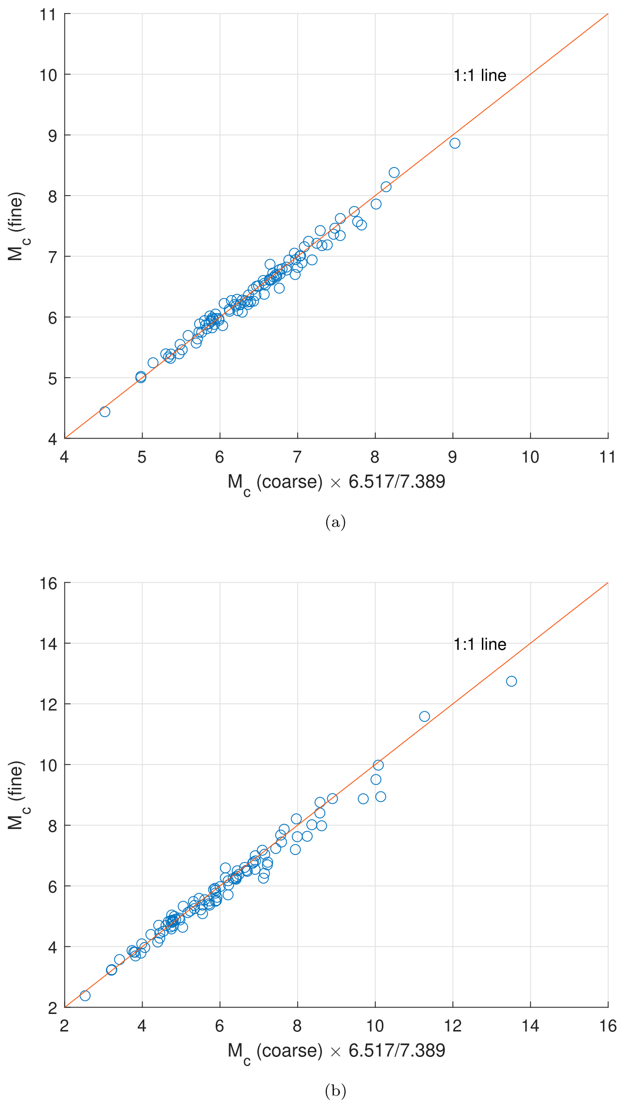

Figure 2. M_c based on the coarse mesh versus M_c based on the fine mesh for $\theta_{\ln c_u} = 2.0$ m ($N = 100$): (a) COV = 0.2; (b) COV = 0.5.

Figure 3. Soil spatial variability for a typical realisation (soil domain $5 \times 5 \times 2$ m and $\theta_{\ln c_u} = 2$ m).

3. Worst-case scale of fluctuation

Figure 4 shows the simulated mean M_c as a function of SOF, for all COV values considered, together with the corresponding lower and upper bounds as the SOF becomes infinitely small and large. It is seen that they all show a (local) minimum value at an intermediate SOF. Li et al. (2021) showed that for smaller SOFs approaching zero, the mean M_c approaches the value based on the median (i.e. $\mu_{c_u}/\sqrt{1+v_c^2}$, a function of COV), and for larger SOFs, on the other hand, the mean M_c values all approach the value based on the mean. A local maximum is also observed, which can be explained by a theoretical evaluation and the weakest link behaviour in the RFEM simulation (Li et al. 2021). So, according to the first definition of a worst-case SOF (i.e. based on the mean soil response), there are some

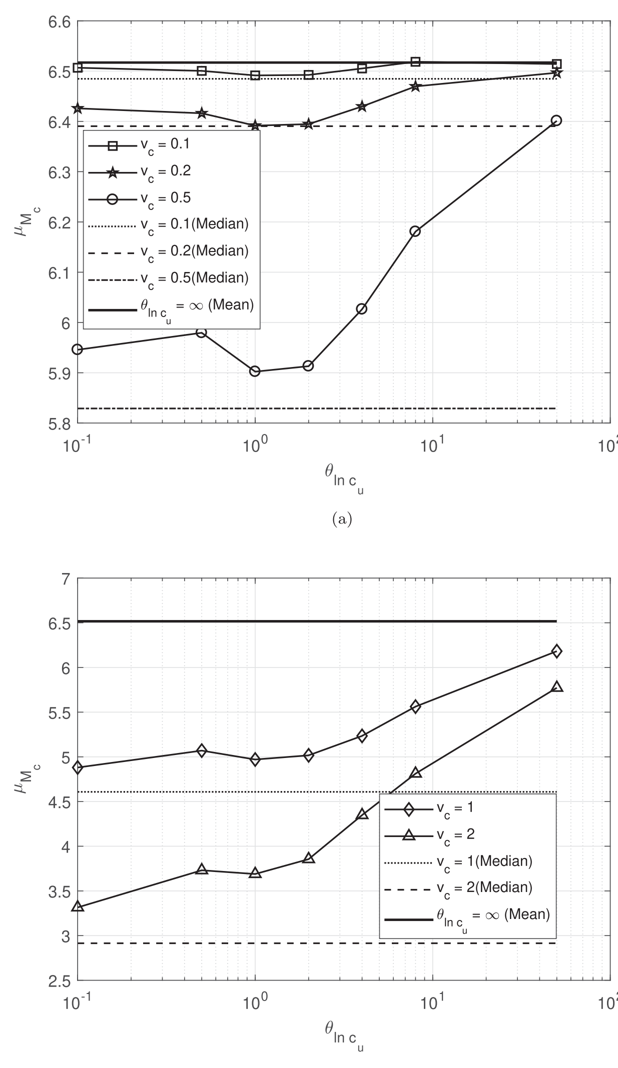

Figure 4. μ_{M_c} versus $\theta_{\ln c_u}$ (lower and upper bounds based on median and mean indicated as lines without markers): (a) COV = 0.1, 0.2, 0.5; (b) COV = 1.0, 2.0.

critical SOFs that lead to a (local) minimum mean response, compared to the mean-based upper bounds when $\theta_{\ln c_u}$ becomes infinity. Note that the current investigation increases the MC number to $N = 600$ in order to improve the estimation accuracy, compared to the previous $N = 200$ in an earlier study (Li et al. 2021). For instance the standard error for the mean estimation of $\mu_{M_c} = 6.40$ is $\sigma_{M_c}/\sqrt{N} = 0.12$ when COV $= 0.5$ and $\theta_{\ln c_u} = 50$ m, which is the case where more realisations are appropriate due to the influence of increasing σ_{M_c} for an increasingly larger SOF, as compared to cases involving smaller SOFs and COVs. This level of accuracy is believed to be reasonably good for all SOFs considered, given the computational cost of a 3D non-linear plastic finite element analysis. In addition, Chwała (2019) observed a similar worst-case SOF for the special case of a square footing, although a different approach based on spatial averaging and kinematic failure mechanisms was used. In the case of rectangular footings, the square footing width in the current investigation may be considered as an equivalence with regard to the footing area.

The second definition of a worst-case SOF is based on the maximum value of the probability of failure (p_f), which may be defined as

$$p_f = P\left[q_f \leq \frac{q_f^d}{F}\right] = P\left[\frac{q_f}{\mu_{c_u}} \leq \frac{N_c'}{F}\right] = P\left[M_c \leq \frac{N_c'}{F}\right]$$
$$= P\left[\ln M_c \leq \ln\frac{N_c'}{F}\right] = \Phi\left(\frac{\ln\frac{N_c'}{F} - \mu_{\ln M_c}}{\sigma_{\ln M_c}}\right) \quad (2)$$

where $q_f^d = \mu_{c_u} N_c'$, N_c' is the deterministic bearing capacity factor (which is 6.517 in this case), F is a given factor of safety and Φ is the standard normal cumulative distribution function. The Monte Carlo simulation to compute p_f consists of the steps shown in Figure 5.

As seen above, p_f is directly related to the two moments of the logarithm of M_c, so it would be informative to know how the mean of $\ln M_c$ changes as a function of SOF. Figure 6 shows these plots for various values of COV. Again, there are minimum mean $\ln M_c$ values for intermediate SOFs. However, a close inspection of these critical SOFs indicates that they have different values to those found in Figure 4. The critical values (i.e. based on the mean response $\mu_{\ln M_c}$ or μ_{M_c}) from Figures 4 and 6 are listed in Table 2. It is seen that they are different for COVs in the range from 1.0 to 2.0.

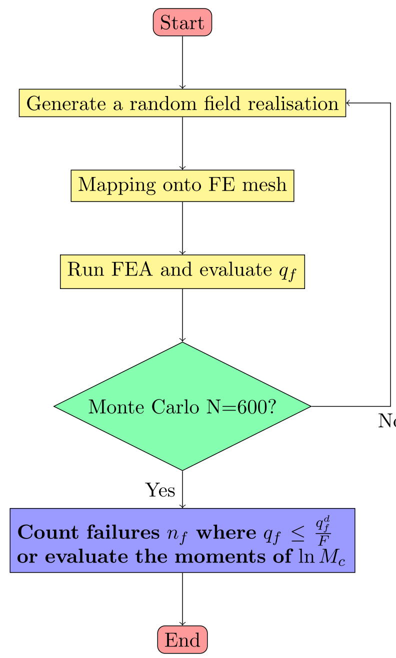

Figure 5. Flowchart for calculating p_f in Equation (2).

Since the variance of $\ln M_c$ also plays a role in the probability calculation, the simulated probability of failure is also investigated and is shown in Figure 7 as a function of SOF for different factors of safety F and two COVs. The worst-case SOF values based on p_f for smaller and larger F values are also listed in Table 2 for comparison (for all COVs considered).

First of all, it is seen that the critical SOF that makes $\mu_{\ln M_c}$ a minimum is not the same as the critical SOF at which μ_{M_c} reaches a (local) minimum, for high values of COV. The critical SOFs where p_f is maximised for smaller F are seen to be approximately equal to the critical SOF values based on $\mu_{\ln M_c}$. While the reason for the latter observation may be obvious, i.e. due to $\mu_{\ln M_c}$ being directly used in the probability equation, the reason for the former observation may not be as obvious. The reason why the former observation might be the case can be explained by the log-normal transformation equations for the two moments of $\ln M_c$ and M_c, i.e.

$$\sigma^2_{\ln M_c} = \ln\left(1 + \frac{\sigma^2_{M_c}}{\mu^2_{M_c}}\right) \quad (3a)$$

$$\mu_{\ln M_c} = \ln \mu_{M_c} - (1/2)\sigma^2_{\ln M_c} \quad (3b)$$

since M_c can be closely approximated by a log-normal distribution (as q_f can be closely approximated by a log-normal distribution due to the assumption that c_u follows a log-normal distribution). A look at Equation

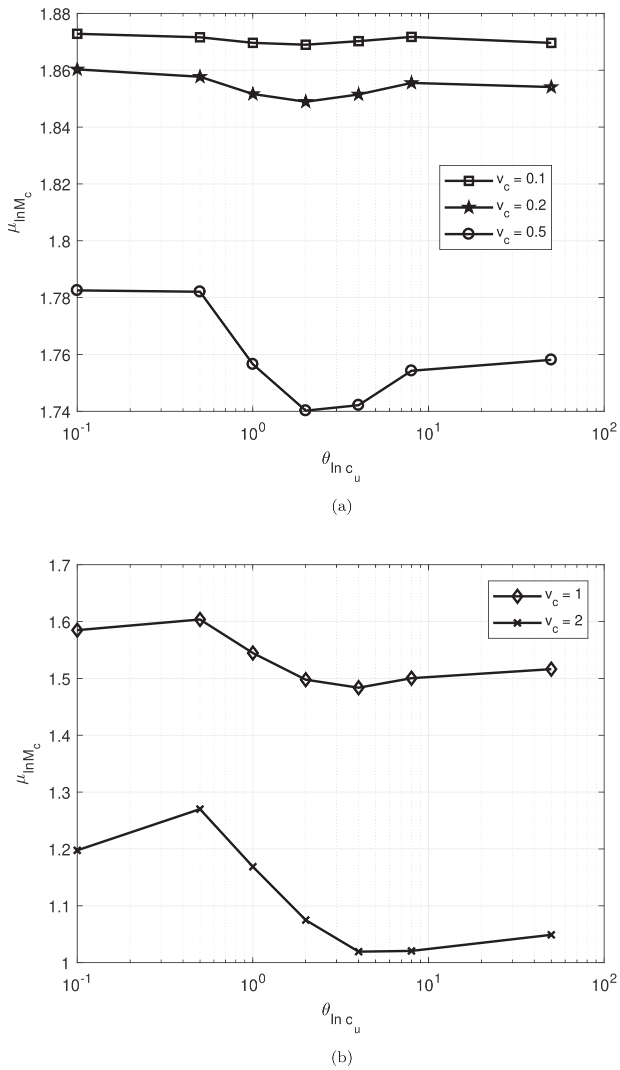

Figure 6. $\mu_{\ln M_c}$ versus $\theta_{\ln c_u}$: (a) COV = 0.1, 0.2, 0.5; (b) COV = 1.0, 2.0.

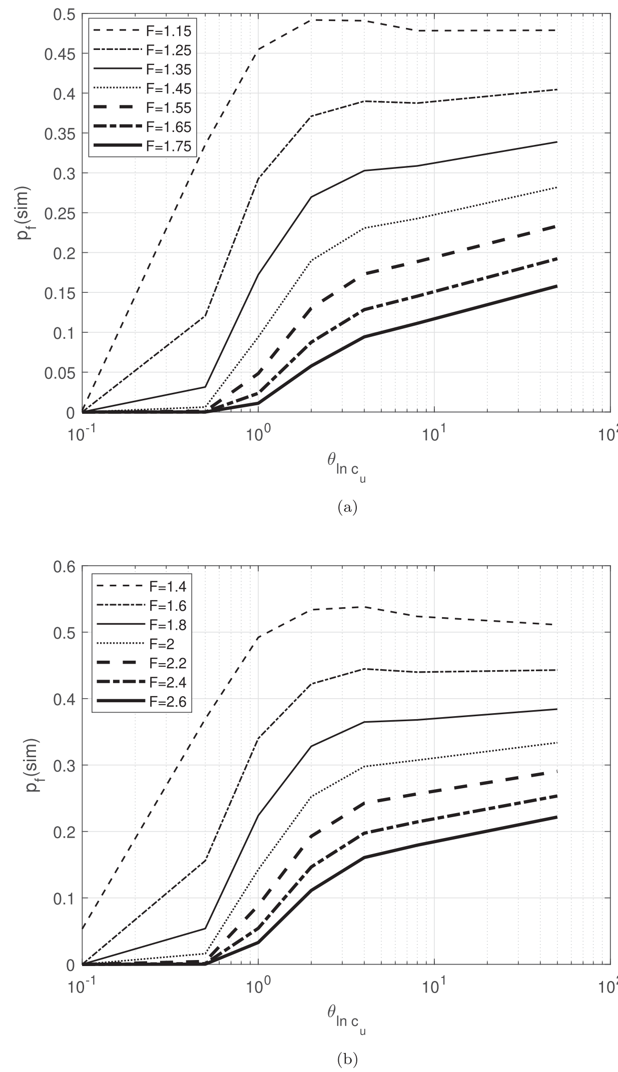

Figure 7. Simulated probabilities versus SOF for different F (relative to deterministic q_f) and COV: (a) COV = 0.5; (b) COV = 1.0.

Table 2. Critical $\theta_{\ln c_u}$ (in metres) from RFEM simulations (B = 1.0 m).

COV	Based on $\mu_{\ln M_c}$	Based on μ_{M_c}	Based on p_f (smaller F)	Based on p_f (larger F)
0.1	2	1–2	–	≥50
0.2	2	1–2	2–4	≥50
0.5	2	1–2	2–4	≥50
1.0	4	1	2–4	≥50
2.0	4	1	2–4	≥50

(3) shows that when evaluating $\mu_{\ln M_c}$, the variance of M_c, $\sigma^2_{M_c}$, also comes into play. That is, the mean, $\mu_{\ln M_c}$, is reduced more by the variance at a higher value of SOF, for higher COVs (compare Figure 6 with Figure 4), so that a larger critical SOF based on $\mu_{\ln M_c}$ may be observed (see also Puła and Griffiths 2021 for the dependency on the coefficient of variation of M_c).

Based on these observations, two things need to be stressed: firstly, the critical SOF may be different in the original space (i.e. lognormally distributed M_c) from that in the logarithmic space (i.e. normally distributed $\ln M_c$); secondly, the critical SOF may be better defined based on the probability of failure as the ultimate goal is probability-based design (i.e. the critical SOF based on the mean logarithmic response should be used). Having said that, the COV values may not be as high as 1.0–2.0 in practice due to some level of site sampling often being available in any design. This availability of site data would in most cases reduce the statistical uncertainties associated with limited information, thereby to some extent separating the true COV due to spatial variability from the total COV that includes statistical uncertainties (Phoon and Kulhawy 1999). The use of the higher COVs in this paper is for those cases where information is limited and insufficient. So, in practice, the two critical SOFs based on mean responses ($\mu_{\ln M_c}$ and μ_{M_c}) and the critical

SOF based on p_f (for smaller F) would not be that different for COV values typically ranged from 0.1 to 0.5.

Another issue arises when one looks at the maximum p_f (for smaller F) for the critical (intermediate) SOFs in Figure 7; they are all roughly in the range of $p_f = 40-60\%$. This seems to make the idea of a critical SOF less valuable, as the target probability of failure is often around 5% or less depending on the importance of different structures constructed on the soil (or nearby), and a relatively high factor of safety is required to satisfy this target probability. For example, a factor of safety of $F = 1.2$, 1.4 or 2.0 (or larger) may be required for COV = 0.1, 0.2 and 0.5, respectively. However, there are no peaks at some intermediate SOF values for the probability curves for these higher F values (the larger the SOF, the greater p_f, with similar trends having been observed in Puła and Chwała (2018) for bearing capacity and Li, Hicks, and Nuttall (2015) and Zhu, Griffiths, and Fenton (2018) for slope stability). That is, the critical SOF may be larger than that observed for smaller F values where a peak is observed at some intermediate SOF value (see Table 2). This implies that in practice, a higher SOF (than the critical SOF observed for smaller F) may need to be conservatively assumed in order for p_f to be within the target level of around 5% (i.e. for higher F), thus also implying a random variable approach assuming an infinite SOF could have been sufficient (Griffiths and Fenton 2004).

The above is true (i.e. the single random variable approach would have been sufficient) without directly using any samples from a site. With consideration of sampling, for high SOFs, the conditional random field would have a very small variance and a mean very close to the input mean. The resultant p_f for practically high F values would then be effectively zero. Note that, on the other hand, when the SOF is small, the random field simulation satisfies the ergodicity condition, i.e. the statistics from one random field can represent the population statistics. In contrast, when the SOF is large in unconditional random field simulations, the mean from one field can not represent the population mean, neither can the variance from one field represent the population variance. So, for small SOFs, unconditional and conditional simulations do not make much difference, but for large SOFs they do. Hence, in practice, conditional approaches (Fenton, Griffiths, and Williams 2005; Li, Hicks, and Vardon 2016) should always be used where possible. In this case, one would still find a critical (intermediate) SOF where the p_f is largest and within the practical target levels (i.e. generally those lines shown in Figure 7 would have a dramatic drawdown for SOFs at the higher end, making p_f a maximum at some intermediate SOF and around the target level of, say, 5% for higher F). One will generally find that this critical SOF is related to the structure dimensions, e.g. footing width $B = 1.0$ m in this case, and is not excessively different from those values observed based on the above unconditional simulations (for smaller F). To investigate this, an analysis with a conditional approach similar to Fenton, Griffiths, and Williams (2005) has been undertaken.

The "true" or actual (random) bearing capacity, q_f, is assumed in this study to be closely approximated by the reaction load computed in the finite element analysis of each soil realisation. The predicted bearing capacity, q_f^s, depends on an estimate of the effective soil properties based on samples taken in the subsurface around the footing. In this paper, the effective soil property $\bar{c}$ is estimated using only a single "virtual sample" sounding taken at a distance r from the centre of the square footing and the sample consists of the random cells down from the soil surface (see Figure 8). Specifically, virtual sampling means that the estimated soil properties $\bar{c}$ are obtained from each random field realisation as the geometric average of the random cell values from the vertical soil column such that $q_f^s = \bar{c} \times N_c'$. It is assumed that the geometric average estimation is better than the arithmetic average estimation, in accordance with the findings in Li et al. (2021). The Monte Carlo simulation for a particular input combination of COV and SOF proceeds in the following steps:

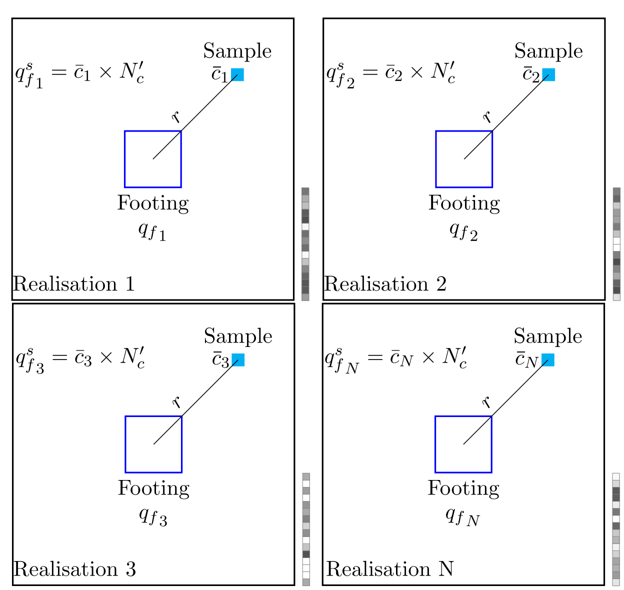

Figure 8. Plan view of the soil domain showing the position of a vertical sample relative to the square footing; the vertical sample consists of $n = 16$ random cells, as shown to the right of each realisation.

1 generate a random field of the undrained shear strength c_u using LAS;
2 map the random local average cells to the integration points within the finite elements;
3 take a virtual sample (such as a CPT sounding) consisting of n random cells along a vertical line at some plan view distance r away from the footing (Figure 8), and compute the effective undrained shear strength $\bar{c}_i = \exp\left(\frac{1}{n}\sum_{j=1}^{n} \ln c_j\right)$ and $q^s_{fi} = \bar{c}_i \times N'_c$;
4 run a finite element analysis to compute the actual bearing capacity q_{fi} of this particular realisation of the spatially varying c_u field;
5 repeat the above steps $N = 600$ times and count the number of realisations that result in $q_{fi} \leq \frac{q^s_{fi}}{F}$.

The procedure differs from those for calculating p_f in Equation (2) in that step (3) is added and q_f is compared to $\frac{q^d_f}{F}$ in step (5). Figure 9 demonstrates this difference in the form of a flowchart with bold text.

In practice, the above can be interpreted as follows: consider the design regulations, which should be applicable to footing designs on similar sites across a region. The sites are similar in that each has the same coefficient of variation of soil properties and the same spatial correlation structure dictated by the same correlation function parametrised by the same SOF. The similar sites involve different realisations of the undrained shear

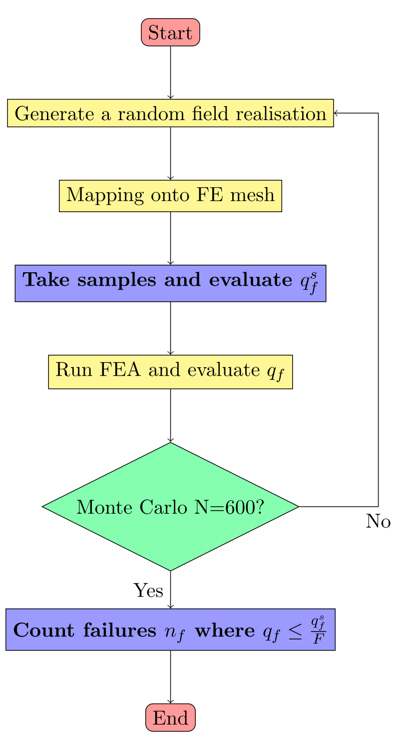

Figure 9. Flowchart for calculating p_f in Equation (4) (the difference to Figure 5 is shown in bold).

strength field, thus they will each have a different estimate $\bar{c}$ obtained by sampling, and thereby a different predicted q^s_f.

The failure probabilities

$$p_f = P\left[q_f \leq \frac{q^s_f}{F}\right] \tag{4}$$

as a function of SOF for various values of F and distance r are plotted in Figure 10 for COV $= 0.5$ and Figure 11 for COV $= 1.0$. (Note that, in a Monte Carlo simulation, $p_f = n_f/N$, where n_f is the number of realisations having a smaller simulated q_f than the predicted q^s_f factored by F, i.e. $q_f \leq \frac{q^s_f}{F}$.) It is seen that, when considering samples, the probability of failure does indeed drop for higher SOF values due to the information provided in the samples (cf. Figure 7 for COV = 0.5 and 1.0). A close look at Figures 10 and 11 indicates that the worst-case SOFs are around the same as those based on the unconditional p_f for smaller F (Figure 7), although the peak in the latter is not as apparent. However, the analysis here at least serves to demonstrate that the "worst-case" SOFs based on an unconditional p_f for smaller F are still useful (they are more or less the same as those based on p_f when taking account of samples). However, whenever it is possible, the conditional approach is preferable. It is also noted that as r starts to increase (i.e. samples moving away from the footing), the probability of failure gets higher for the same factor of safety, which is as expected due to the samples being increasingly less correlated to the soil properties directly below the footing. Note also that for a target p_f of around 5%, the corresponding standard error of the estimation is about $\sqrt{p_f(1-p_f)/N} = 0.9\%$ for $N = 600$. Admittedly this error is not particularly small, but it certainly has improved over the earlier study using $N = 200$. In design simulations, however, a larger number should preferably be used. In this study, the required factor of safety to achieve this level of safety would need to be larger than 1.6 and 1.9 (for COV $= 0.5$ and 1.0, respectively), depending on the site variability and the intensity of site sampling. A factor of safety of 3.1 may be required if a single vertical sample should be taken from a location at the largest distance away from the footing for a relatively highly variable soil.

4. Conclusions

This paper presents some recent observations on the worst-case SOF in the context of 3D square footing stability.

These observations and their implications are listed as follows:

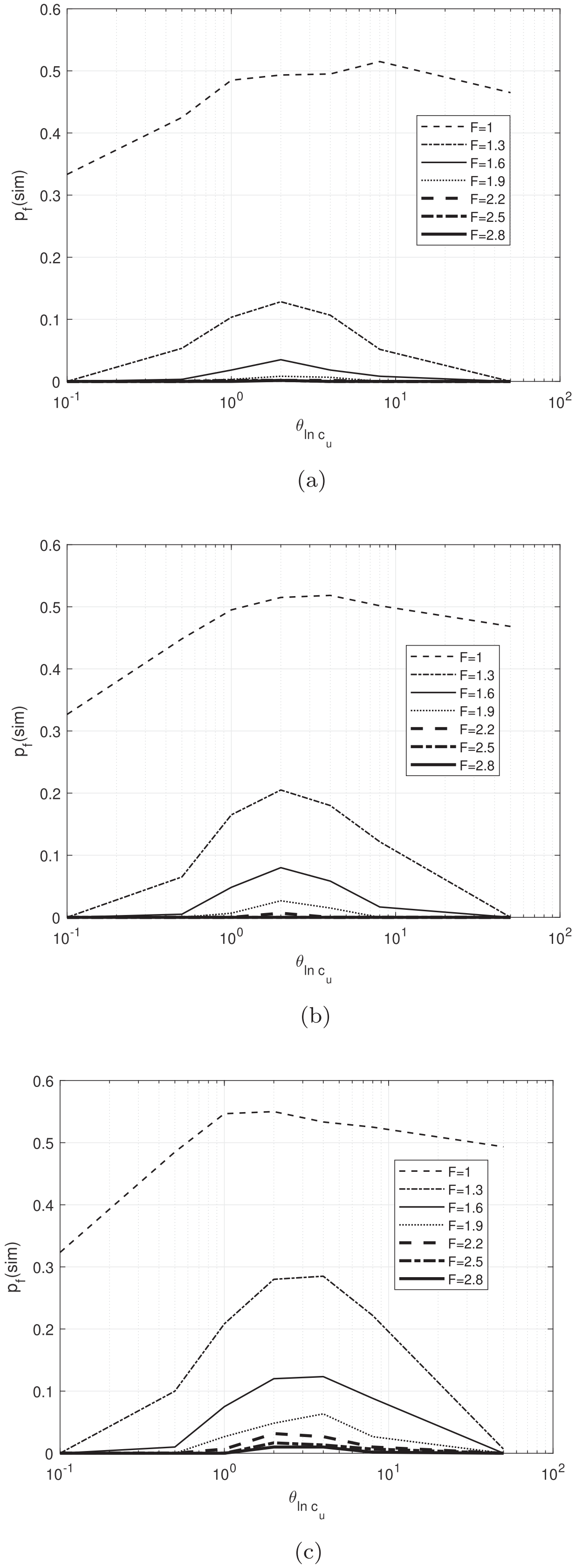

Figure 10. Simulated probabilities versus SOF for different F (relative to q_f^s) and CPT sampling location, COV = 0.5 ($B = 1.0$ m): (a) $r/B = 0$; (b) $r/B = \sqrt{2} \times 0.5$; (c) $r/B = \sqrt{2} \times 1.5$.

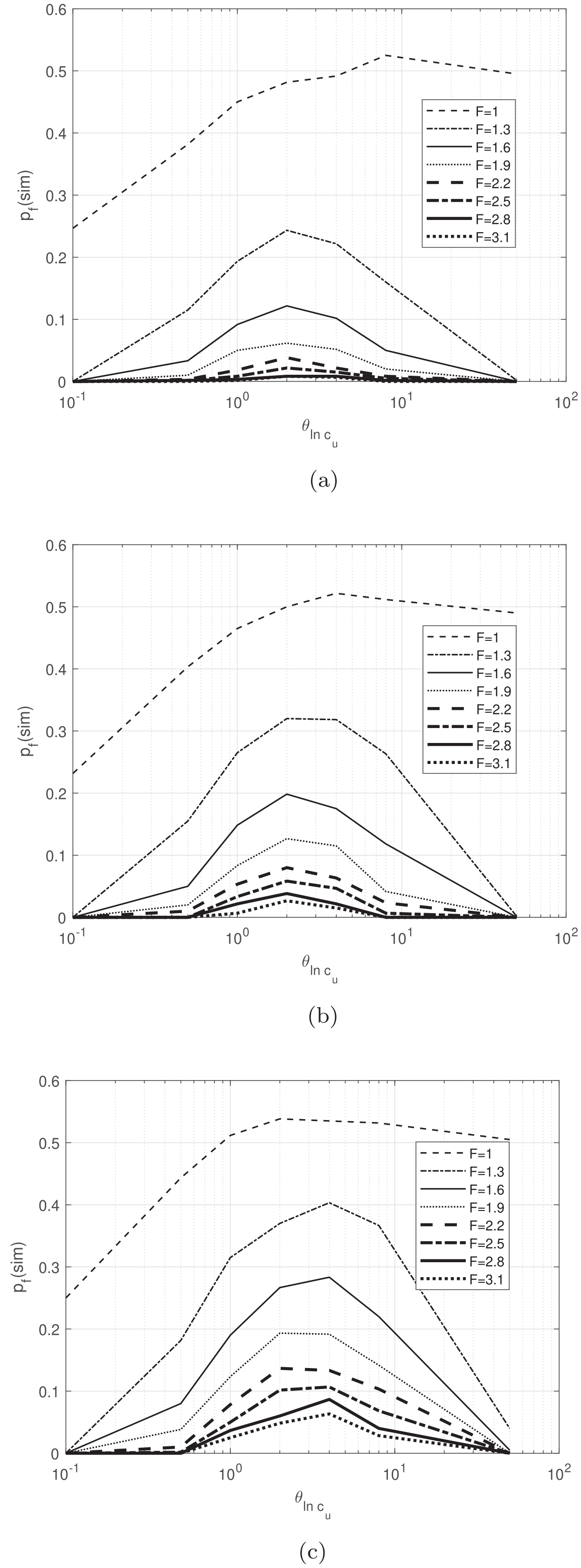

Figure 11. Simulated probabilities versus SOF for different F (relative to q_f^s) and CPT sampling location, COV = 1.0 ($B = 1.0$ m): (a) $r/B = 0$; (b) $r/B = \sqrt{2} \times 0.5$; (c) $r/B = \sqrt{2} \times 1.5$.

(1) The critical SOF is different if it is calculated using the mean response or the log mean response – although at expected values of COV (i.e. 0.1-0.5) they are practically the same.
(2) The critical SOF when determined by the probability of failure without using samples is usually infinite, except when the probability of failure is large, which is not usually the practical case.
(3) The critical SOF is strongly affected by on-site data, which strongly reduces the probability of failure for large SOFs. This leads to a critical SOF being defined at some intermediate value.
(4) With practical values of COV and using on-site data, the critical SOF is between 1 and 4 times the foundation width. Moreover, the data show that at this worst case the stability is reasonably invariant to changes in the SOF; therefore utilising 2 times the footing breadth seems reasonable.

It should be noted that the above observations are based on the assumption of an isotropic correlation structure of soil strength. Soils are generally anisotropically correlated with larger correlation lengths in the horizontal directions. In such cases, due to the vertical SOF being more easily obtained, by fixing the vertical SOF at some certain value the above observations are still believed to be applicable for the horizontal SOF. However, some additional study is necessary to establish the relationship between the worst-case horizontal SOF and the square footing breadth (and for rectangular footings, its relationship to the footing width and length).

Notation

c_u	undrained shear strength;
$\bar{c}$	geometric average of the virtual sample;
n	number of random cells in the vertical sample;
n_f	number of failures, i.e. when $q_f \leq \frac{q_f^s}{F}$;
p_f	probability of failure;
q_f	ultimate bearing capacity;
q_f^d	deterministic ultimate bearing capacity;
q_f^s	ultimate bearing capacity based on samples;
r	distance of sample from footing centre;
V_c	coefficient of variation (COV);
$\boldsymbol{x}, \boldsymbol{x}'$	spatial locations;
B	footing width;
E	Young's modulus;
F	factor of safety;
M_c	stochastic bearing capacity factor;
N	number of Monte Carlo realisations;
N_c'	deterministic bearing capacity factor;
$P[-]$	probability of an event;
$\theta_{\ln c_u}$	scale of fluctuation of $\ln c_u$;
μ	mean value of a subscripted variable;
v	Poisson's ratio;
σ	standard deviation of a subscripted variable;
$\theta_{\ln c_u}^v$	vertical scale of fluctuation;
$\theta_{\ln c_u}^h$	horizontal scale of fluctuation;
$\boldsymbol{\tau}$	separation distance vector $(= \boldsymbol{x} - \boldsymbol{x}')$;
τ_1, τ_2, τ_3	separation distances in the three coordinate directions;
Φ	standard normal cumulative distribution function.

Disclosure statement

No potential conflict of interest was reported by the author(s).

Funding

This work was supported by the National Natural Science Foundation of China under Grant number 41807228 and the Fundamental Research Funds for the Central Universities under Grant number 2652019321.

ORCID

Yajun Li http://orcid.org/0000-0002-5863-5821
Philip J. Vardon http://orcid.org/0000-0001-5614-6592
Michael A. Hicks http://orcid.org/0000-0002-7603-7040

References

Allahverdizadeh, P., D. V. Griffiths, and G. A. Fenton. 2015. "The Random Finite Element Method (RFEM) in Probabilistic Slope Stability Analysis with Consideration of Spatial Variability of Soil Properties." In International Foundations Congress and Equipment Expo (IFCEE) 2015, Texas, USA, 1946–1955.

Baecher, G. B., and T. S. Ingra. 1981. "Stochastic FEM in Settlement Predictions." *Journal of the Geotechnical Engineering Division* 107 (4): 449–463.

Cami, B., S. Javankhoshdel, K.-K. Phoon, and J. Ching. 2020. "Scale of Fluctuation for Spatially Varying Soils: Estimation Methods and Values." *ASCE-ASME Journal of Risk and Uncertainty in Engineering Systems, Part A: Civil Engineering* 6 (4): 03120002.

Ching, Jianye, Kok-Kwang Phoon, and Shung-Ping Sung. 2017. "Worst Case Scale of Fluctuation in Basal Heave Analysis Involving Spatially Variable Clays." *Structural Safety* 68: 28–42.

Christian, J. T., and G. B. Baecher. 2003. "Probabilistic Foundation Settlement on Spatially Random Soil. Discussion and Closure." *Journal of Geotechnical and Geoenvironmental Engineering* 129 (9): 866–867.

Chwała, Marcin. 2019. "Undrained Bearing Capacity of Spatially Random Soil for Rectangular Footings." *Soils and Foundations* 59 (5): 1508–1521.

De Gast, Tom, Philip J. Vardon, and Michael A. Hicks. 2021. "Assessment of Soil Spatial Variability for Linear Infrastructure Using Cone Penetration Tests." *Géotechnique* 71 (11): 999–1013.

Fenton, Gordon A. 1999. "Random Field Modeling of CPT Data." *Journal of Geotechnical and Geoenvironmental Engineering* 125 (6): 486–498.

Fenton, Gordon A., and D. V. Griffiths. 1996. "Statistics of Free Surface Flow Through Stochastic Earth Dam." *Journal of Geotechnical Engineering* 122 (6): 427–436.

Fenton, Gordon A., and D. V. Griffiths. 2002. "Probabilistic Foundation Settlement on Spatially Random Soil." *Journal of Geotechnical and Geoenvironmental Engineering* 128 (5): 381–390.

Fenton, Gordon A., and D. V. Griffiths. 2003. "Bearing-Capacity Prediction of Spatially Random c–φ Soils." *Canadian Geotechnical Journal* 40 (1): 54–65.

Fenton, Gordon A., and D. Vaughan Griffiths. 2008. *Risk Assessment in Geotechnical Engineering*. New York: John Wiley & Sons.

Fenton, Gordon A., D. V. Griffiths, and W. Cavers. 2005. "Resistance Factors for Settlement Design." *Canadian Geotechnical Journal* 42 (5): 1422–1436.

Fenton, Gordon A., D. V. Griffiths, and M. B. Williams. 2005. "Reliability of Traditional Retaining Wall Design." *Geotechnique* 55 (1): 55–62.

Fenton, Gordon A., D. V. Griffiths, and Xianyue Zhang. 2008. "Load and Resistance Factor Design of Shallow Foundations Against Bearing Failure." *Canadian Geotechnical Journal* 45 (11): 1556–1571.

Fenton, Gordon A., G. M. Paice, and D. V. Griffiths. 1996. "Probabilistic Analysis of Foundation Settlement." In Proceedings of Uncertainty in the Geologic Environment: From Theory to Practice, Madison, USA, 651–665. ASCE.

Fenton, Gordon A., and Erik H. Vanmarcke. 1990. "Simulation of Random Fields Via Local Average Subdivision." *Journal of Engineering Mechanics* 116 (8): 1733–1749.

Fenton, Gordon A., Xianyue Zhang, and D. V. Griffiths. 2007. "Reliability of Shallow Foundations Designed Against Bearing Failure Using LRFD." *Georisk: Assessment and Management of Risk for Engineered Systems and Geohazards* 1 (4): 202–215.

Fenton, Gordon A., Haiying Zhou, Mark B. Jaksa, and D. V. Griffiths. 2003. "Reliability Analysis of a Strip Footing Designed Against Settlement." In 9th International Conference of Applications of Statistics and Probability in Civil Engineering, California, USA, 1271–1277.

Griffiths, D. V., and Gordon A. Fenton. 1998. "Probabilistic Analysis of Exit Gradients Due to Steady Seepage." *Journal of Geotechnical and Geoenvironmental Engineering* 124 (9): 789–797.

Griffiths, D. V., and Gordon A. Fenton. 2004. "Probabilistic Slope Stability Analysis by Finite Elements." *Journal of Geotechnical and Geoenvironmental Engineering* 130 (5): 507–518.

Griffiths, D. V., Gordon A. Fenton, and Heidi R. Ziemann. 2008. "Reliability of Passive Earth Pressure." *Georisk: Assessment and Management of Risk for Engineered Systems and Geohazards* 2 (2): 113–121.

Hicks, Michael A., and Kristinah Samy. 2002. "Influence of Heterogeneity on Undrained Clay Slope Stability." *Quarterly Journal of Engineering Geology and Hydrogeology* 35 (1): 41–49.

Huang, J., and D. V. Griffiths. 2015. "Determining An Appropriate Finite Element Size for Modelling the Strength of Undrained Random Soils." *Computers and Geotechnics* 69: 506–513.

Jaksa, M. B., W. S. Kaggwa, and P. I. Brooker. 1999. "Experimental Evaluation of the Scale of Fluctuation of a Stiff Clay." In Proceedings of the 8th International Conference on Applications of Statistics and Probability, Sydney, Australia, 415–422.

Li, Dianqing, Z. Cao, Jianye Ching, S. Dasaka, Jinsong Huang, Mark Jaksa, Shin-ichi Nishimura, Armin Stuedlein, and Giovanna Vessia. 2017. "Incorporating Spatial Variability Into Geotechnical Reliability Based Design." In Joint TC205/TC304 Working Group on "Discussion of Statistical/reliability Methods for Eurocodes", 135–156.

Li, Y. J., G. A. Fenton, M. A. Hicks, and N. X. Xu. 2021. "Probabilistic Bearing Capacity Prediction of Square Footings on 3D Spatially Varying Cohesive Soils." *Journal of Geotechnical and Geoenvironmental Engineering* 147 (6): 04021035.

Li, Y. J., M. A. Hicks, and J. D. Nuttall. 2015. "Comparative Analyses of Slope Reliability in 3D." *Engineering Geology* 196: 12–23.

Li, Y. J., M. A. Hicks, and P. J. Vardon. 2016. "Uncertainty Reduction and Sampling Efficiency in Slope Designs Using 3D Conditional Random Fields." *Computers and Geotechnics* 79: 159–172.

Li, Y. J., Kang Liu, Bin Zhang, and N. X. Xu. 2020. "Reliability of Shape Factors for Bearing Capacity of Square Footings on Spatially Varying Cohesive Soils." *International Journal of Geomechanics* 20 (3): 04019195.

Lundberg, A. B., and Y. J. Li. 2015. "Probabilistic Characterization of a Soft Scandinavian Clay Supporting a Light Quay Structure." In *Proceedings of the 5th International Symposium on Geotechnical Safety and Risk*, 170–175. Rotterdam, Netherlands.

Meyerhof, G. G. 1951. "The Ultimate Bearing Capacity of Foudations." *Geotechnique* 2 (4): 301–332.

Phoon, Kok-Kwang, and Fred H. Kulhawy. 1999. "Characterization of Geotechnical Variability." *Canadian Geotechnical Journal* 36 (4): 612–624.

Puła, Wojciech, and Marcin Chwała. 2018. "Random Bearing Capacity Evaluation of Shallow Foundations for Asymmetrical Failure Mechanisms with Spatial Averaging and Inclusion of Soil Self-Weight." *Computers and Geotechnics* 101: 176–195.

Puła, W., and D. V. Griffiths. 2021. "Transformations of Spatial Correlation Lengths in Random Fields." *Computers and Geotechnics* 136: 104151.

Puła, W., J. M. Pieczyńska-Kozłowska, and M. Chwała. 2017. "Search for the Worst-Case Correlation Length in the Bearing Capacity Probability of Failure Analyses." In Geo-Risk 2017, Colorado, USA, 534–544.

Smith, I. M., and D. V. Griffiths. 2005. *Programming the Finite Element Method*. New York: John Wiley & Sons.

Spencer, W. A. 2007. "Parallel Stochastic and Finite Element Modelling of Clay Slope Stability in 3D." PhD diss., University of Manchester, Manchester, UK.

Tabarroki, Mohammad, and Jianye Ching. 2019. "Discretization Error in the Random Finite Element Method for Spatially Variable Undrained Shear Strength." *Computers and Geotechnics* 105: 183–194.

Vanmarcke, Erik H. 1977. "Probabilistic Modeling of Soil Profiles." *Journal of the Geotechnical Engineering Division* 103 (11): 1227–1246.

Vanmarcke, Erik H. 1978. "Probabilistic Characterization of Soil Profiles." In *Site Characterization & Exploration*, 199–219. Evanston, Illinois, USA: ASCE.

Vanmarcke, E. H. 1983. *Random Fields: Analysis and Synthesis*. Cambridge, MA: MIT Press.

Vessia, Giovanna, Yan-Guo Zhou, Andy Leung, Wojciech Pula, Diego Di Curzio, Mohammad Tabarroki, and Jianye Ching. 2021. "Numerical Evidences for Worst-Case Scale of Fluctuation." In State-Of-The-Art Review of Inherent Variability and Uncertainty in Geotechnical Properties and Models, 204.

Zhu, D., D. V. Griffiths, and G. A. Fenton. 2018. "Worst-Case Spatial Correlation Length in Probabilistic Slope Stability Analysis." *Géotechnique* 69 (1): 85–88.